



Published in final edited form as:

*J Nucl Cardiol.* 2021 August ; 28(4): 1395–1408. doi:10.1007/s12350-019-01811-y.

## Reducing radiation dose from myocardial perfusion imaging in subjects with complex congenital heart disease

Sara L. Partington, MD<sup>a</sup>, Anne Marie Valente, MD<sup>b,c</sup>, John Bruyere Jr, MD<sup>d</sup>, Dillenia Rosica, MD<sup>d</sup>, Keri M. Shafer, MD<sup>b,c</sup>, Michael J. Landzberg, MD<sup>b,c</sup>, Viviany R. Taqueti, MD<sup>d</sup>, Ron Blankstein, MD<sup>d</sup>, Hicham Skali, MD<sup>d</sup>, Neha Kwatra, MD<sup>e</sup>, Marcelo F. DiCarli, MD<sup>d,f</sup>, Frederick D. Grant, MD<sup>e</sup>, Sharmila Dorbala, MD, MPH<sup>d,f</sup>

<sup>a</sup>Division of Cardiology, Department of Medicine, Hospital of the University of Pennsylvania and Children's Hospital of Philadelphia, Philadelphia

<sup>b</sup>Department of Cardiology, Boston Children's Hospital, Boston

<sup>c</sup>Division of Medicine, Department of Cardiology, Brigham and Women's Hospital, Boston

<sup>d</sup>Cardiovascular Imaging Program, Departments of Medicine (Cardiovascular Division) and Radiology, Brigham and Women's Hospital, Boston

<sup>e</sup>Division of Nuclear Medicine, Department of Radiology, Boston Children's Hospital, Boston

<sup>f</sup>Division of Nuclear Medicine and Molecular Imaging, Department of Radiology, Brigham and Women's Hospital, Harvard Medical School, Boston, MA

### Abstract

**Introduction.**—The prevalence of defects and effective radiation dose from various myocardial perfusion imaging (MPI) strategies in congenital heart disease (CHD) is unknown.

**Methods.**—We studied 75 subjects with complex CHD (ages 5 to 80 years) referred for MPI between 2002 and 2015. A rest and exercise or pharmacologic stress MPI was performed using <sup>99m</sup>Tc sestamibi, <sup>82</sup>Rb or <sup>13</sup>N-ammonia, and Sodium iodide SPECT (single-photon emission computed tomography), SPECT/CT or Cadmium zinc telluride (CZT) SPECT or PET (positron emission tomography)/CT scanners. Deidentified images were interpreted semi-quantitatively in three batches: stress only MPI, stress/rest MPI, and stress/rest MPI with taking into account a history of ventricular septal defect repair. Effective radiation dose was estimated for stress/rest MPI and predicted for 1-day stress-first (normal stress scans), and for 2-day stress/rest MPI (abnormal stress scans).

---

Reprint requests: Sharmila Dorbala, MD, MPH, Division of Nuclear Medicine and Molecular Imaging, Department of Radiology, Brigham and Women's Hospital, Harvard Medical School, 75 Francis Street, Boston, MA 02115, USA; sdorbala@partners.org 1071-3581/\$34.00.

**Electronic supplementary material** The online version of this article (<https://doi.org/10.1007/s12350-019-01811-y>) contains supplementary material, which is available to authorized users.

The authors of this article have provided a PowerPoint file, available for download at SpringerLink, which summarises the contents of the paper and is free for re-use at meetings and presentations. Search for the article DOI on SpringerLink.com.

**Publisher's Note** Springer Nature remains neutral with regard to jurisdictional claims in published maps and institutional affiliations.

**Results.**—The median age was 18.6 years. The most common type of CHD was transposition of the great arteries (63%). Rest/stress MPI was abnormal in 43% of subjects and 25% of the abnormal scans demonstrated reversible defects. Of the subjects with abnormal MPI, 33% had significant underlying anatomic coronary artery obstruction. Estimated mean effective radiation dose ranged from  $2.1 \pm 0.6$  mSv for  $^{13}\text{N}$ -ammonia PET/CT to  $12.5 \pm 0.9$  mSv for SPECT/CT. Predicted effective radiation dose was significantly lower for stress-first MPI and for 2-day stress/rest protocols.

**Conclusions.**—Due to the relatively high prevalence of abnormal stress MPI, tailored protocols with a stress-first MPI as well as the use of 2-day protocols and advanced imaging technologies including CZT SPECT, novel image reconstruction software, and PET MPI could substantially reduce radiation dose in complex CHD.

### Keywords

Complex congenital heart disease; Radiation; SPECT; PET; Myocardial perfusion imaging

---

## INTRODUCTION

Over 1.4 million adults in the United States were estimated to have congenital heart disease in 2010,<sup>1</sup> and the prevalence of adults with complex congenital heart disease (complex CHD) continues to increase.<sup>2</sup> As individuals with complex CHD age, they are at greater risk for atherogenic risk factors than the general population<sup>3</sup> predisposing them to coronary atherosclerosis.<sup>4,5</sup> Risk of ischemia is also increased from a multitude of non-atherogenic processes<sup>6</sup> such as mechanical obstruction of coronary arteries from congenital coronary anomalies, compression from abnormal cardiac structures or implanted devices,<sup>7</sup> or coronary ostial fibrointimal proliferation and kinking from prior coronary artery reimplantation.<sup>8,9</sup> As with the general population, individuals with CHD are at risk for non-cardiac chest pain making non-invasive testing for myocardial ischemia a reasonable diagnostic strategy in those with complex CHD and an intermediate risk of myocardial ischemia.

Despite the availability of several advanced stress imaging modalities, such as echocardiography, cardiac magnetic resonance (CMR) imaging, and radionuclide imaging, the choice of stress technique and imaging modality for ischemia evaluation in complex CHD is not standardized. Due to the concern of mechanical obstruction of coronary arteries in many individuals with complex CHD, exercise, as opposed to pharmacologic stress, is preferred.<sup>6</sup> Radionuclide myocardial perfusion imaging (MPI) offers the advantages of exercise stress (compared to CMR which requires pharmacologic stress), and high-resolution MPI even in individuals with complex cardiac anatomy (compared to echocardiography which is often limited by spatial resolution and image quality).<sup>6</sup> However, literature on the utility of stress radionuclide MPI in the management of individuals with complex CHD is limited.

Radiation exposure remains an overarching concern with radionuclide MPI, particularly due to the young age of individuals with complex CHD. A recent consensus document from the Image Gently Alliance highlighted the relatively high cumulative lifetime burden of ionizing radiation in children with complex CHD, from the multiple imaging studies and procedures

over their lifetimes,<sup>10</sup> and emphasized the need to achieve high-quality studies with the lowest achievable radiation dose. Novel radionuclide scanners including high-sensitivity semiconductor detector single-photon emission computed tomography (SPECT) scanners, positron emission tomography (PET),<sup>11</sup> novel image reconstruction software,<sup>12,13</sup> and novel imaging protocols including stress-first imaging,<sup>14</sup> substantially lower radiation dose from MPI.<sup>15</sup> Radiation dose savings from these novel dose reduction methods have not yet been evaluated in complex CHD.

Our study in children and adults with complex CHD had the following aims: (1) to estimate the effective radiation dose from novel and conventional MPI strategies; (2) to propose methods to reduce radiation dose for MPI in complex CHD.

## METHODS

We studied 75 consecutive subjects of ages 5–80 years old with a history of surgically repaired complex CHD involving conotruncal anomalies and single ventricular physiology who underwent stress radionuclide MPI for clinical indications between the years of 2002 and 2015. We included subjects with CHD of great complexity as well as subjects with tetralogy of Fallot which is in the moderate severity category based on CHD taskforce criteria.<sup>1</sup> These types of CHD were included in this study since these conditions were considered to involve structural lesions that may alter perfusion patterns in MPI independent of coronary artery abnormalities. Subjects were identified using the Research Subject Data Registry at the adult hospital (Brigham and Women's Hospital, Boston, MA) querying ICD-9 codes for various types of conotruncal and single ventricle congenital heart diseases, adult congenital heart disease ordering providers, and MPI study codes. Subjects meeting the same inclusion criteria at the pediatric hospital (Boston Children's Hospital, Boston, MA) between 2006 and February 2013 were identified. For subjects with more than one study, only the most recent study was analyzed. This study was approved by the institutional review board of Brigham and Women's Hospital (Partners) and Boston Children's Hospital.

### Clinical Data

Subject demographics, type of complex CHD, surgical repairs, atherogenic coronary risk factors, cardiac symptoms, medications, reason for test, prior ischemic testing, and coronary artery imaging with invasive coronary angiography or coronary CT angiography were systematically recorded from medical records. Atherogenic coronary risk factors and associated complex CHD abnormalities that were not documented in the medical records were assumed to be absent.

### Stress Testing

At the adult hospital, stress was performed with treadmill exercise using a Bruce protocol or with pharmacologic stress. Pharmacologic stress was performed using vasodilator stress (dipyridamole, adenosine or regadenoson) or with inotropic stress (dobutamine) using standard protocols. At the children's hospital, subjects underwent treadmill or bicycle ergometer stress. Concurrent cardiopulmonary testing as described in a prior publication<sup>16</sup> was also occasionally performed with MPI at the children's hospital. Exercise

time, symptoms, rest and exercise hemodynamics, as well as ST changes were recorded prospectively. In subjects undergoing bicycle ergometer stress and/or VO<sub>2</sub> testing, workload and VO<sub>2</sub> were recorded, respectively.

### Acquisition of Myocardial Perfusion Images

MPI was performed per standard protocols using SPECT or PET. At the adult hospital, SPECT studies were performed with <sup>99m</sup>Tc-sestamibi with 4.5–12 mCi for rest and 15–34 mCi for stress (after 2001) using weight-based dosing (ranges of patient weights with associated <sup>99m</sup>Tc-sestamibi dosages). Images were acquired 15–45 minutes after injection of radiotracer with a two-headed SPECT gamma camera (ECAM, Siemen's Medical Solutions, USA), SPECT/CT gamma camera (Symbia T-6, Siemen's medical Solutions, USA), or a CZT (cadmium zinc telluride) scanner (DSPECT, Spectrum Dynamics, Israel). At the pediatric hospital, subjects received <sup>99m</sup>Tc-sestamibi 0.150 mCi/kg for rest and 0.350 mCi/kg for stress. Images were acquired 15–45 minutes after exercise with a two-headed SPECT gamma camera (ECAM, Siemen's Medical Solutions, USA).

<sup>82</sup>Rubidium or <sup>13</sup>N-ammonia PET/CT scans were acquired with a GE Discovery LS PET/CT or Siemens Biograph PET/CT and standard protocols. <sup>82</sup>Rubidium PET was performed at rest and following pharmacological stress with  $46.1 \pm 9.3$  mCi and  $46.1 \pm 9.3$  mCi of <sup>82</sup>Rubidium, respectively, in a 2D mode. <sup>13</sup>N-ammonia PET was performed with  $7.3 \pm 3.6$  mCi and  $8.6 \pm 2.5$  mCi of <sup>13</sup>N-ammonia, respectively, at rest and following exercise stress in a 3D mode.

### Analysis of Myocardial Perfusion Images

All original images were reformatted again using Invia software (University of Michigan 4DM software, Ann Arbor, MI) and deidentified with a study ID number. Myocardial perfusion of the systemic ventricle was assessed (as opposed to interpretation of the anatomical left ventricle or the left-sided ventricle). The myocardial perfusion images were scored visually with a semi-quantitative method using a 0–4 score (0 = normal, 4 = absent tracer uptake) and a 17-segment heart model.<sup>17</sup> Summed stress, rest, and difference scores were calculated.<sup>18</sup> A summed stress score of < 4 was considered normal.<sup>19</sup> Automated semi-quantitative computer-based analysis could not be used to assess myocardial perfusion due to the lack of established normal limits databases due to the possible atypical locations of ventricles, outflow tracts, and prosthetic material in complex CHD that may not be consistent with standard algorithms.

Deidentified images were interpreted by an experienced nuclear cardiologist (SD). Myocardial perfusion images were sequentially interpreted in three batches and each batch was analyzed on a different day. In each batch, images were scored blinded to clinical history and scores were finalized after a review of the relevant clinical history. For the first round, the reader assessed only the stress images to replicate results of stress-only imaging, and summed stress score was calculated. For the second round, the reader assessed the stress and rest images and the summed stress, rest, and difference scores were calculated. For the third round, the reader reviewed VSD history and assessed if the perfusion defect could be attributable to the VSD patch. Images were categorized as normal, probably

normal, equivocal, probably abnormal, or abnormal for each batch. All but one of the 75 images were interpretable for systematic and sequential MPI interpretation. The one subject who had images that were challenging to interpret due to image quality was considered equivocal.

### Subpulmonary Ventricle Assessment

Subpulmonary ventricular radiotracer uptake was semi-quantitatively assessed. Subpulmonary ventricular radiotracer uptake has traditionally been useful as a marker for pulmonary hypertension<sup>20,21</sup> but in the congenital heart disease population, it could potentially be helpful for assessing the degree of compensatory subpulmonary ventricular hypertrophy in the setting of outflow tract obstruction to the pulmonary artery. Subpulmonary ventricular uptake was assessed as follows: 0 = no visualization, 1 = visualization but less counts than other ventricle, 2 = counts equal to other ventricle, 3 = counts greater than other ventricle.<sup>20</sup>

### Coronary Angiography

Coronary artery obstruction was defined based on the reports of invasive or CT coronary angiography. A coronary artery narrowing of  $\geq 70\%$  diameter stenosis in left anterior descending, left circumflex, right coronary artery or their branches; and  $\geq 50\%$  in the left main coronary artery from atherosclerosis or extrinsic compression was considered to be a significant obstruction. Coronary artery imaging was considered recent if it was performed within a year of the MPI study.

### Estimation of Effective Radiation Dose

Effective radiation dose from MPI was determined for <sup>99m</sup>Tc-sestamibi using 0.009 mSv/MBq at rest and 0.0079 mSv/MBq at stress; for <sup>13</sup>N-ammonia using 0.0027 mSv/MBq; and for <sup>82</sup>rubidium using 0.0017 mSv/MBq, based on previously published estimations from SNMMI.<sup>22</sup> We also used the SNMMI radiation dosimetry tool for <sup>99m</sup>Tc-sestamibi (<http://wwwsnmmi.org/ClinicalPractice/doseTool.aspx>) which takes into account patient age and gender. For the age-based model, radiation doses for subjects between 5 and 10 years were calculated using the 10-year-old model, and greater than 10 to 15.9 years were calculated using the 15-year-old model. Adult male and adult female models were used for subjects  $\geq 16$  years. For subjects who underwent MPI with a low-dose attenuation correction CT, 0.3 mSv was added for CT dose (0.6 mSv for SPECT/CT and <sup>13</sup>N-ammonia with exercise, when 2 CT scans were performed). In addition to actual doses from this study, we estimated radiation doses for scenarios of stress-only study (using stress radiation dose with CT when applicable, for subjects with a normal stress scan) and 2-day equal radiotracer dose study (using two times rest radiation dose with CT when applicable, for subjects with an abnormal stress scan).

### Statistical Analysis

Data are presented as mean  $\pm$  SD or median  $\pm$  interquartile range (IQR) depending on the distribution of the data for continuous variables and as proportions for discrete variables. Mean effective radiation doses between SPECT, CZT SPECT, SPECT/CT, and

PET/CT were compared using ANOVA and a Bonferroni post hoc test for between-group comparisons. A student's *t*-test was used with a  $P < 0.05$  considered significant when appropriate.

## RESULTS

### Baseline Characteristics

The study cohort included 75 subjects, 65% ( $N = 49$ ) male, with a median age of 18.6 years (IQR 15.1–28.4 years, minimum age 5.1 years, maximum age 76.1 years) at the time of MPI (Table 1). The most common type of CHD was transposition of the great arteries (63%,  $N = 47$ ) with the majority (87%,  $N = 41$ ) having had an arterial switch repair with coronary artery reimplantation (Figure 1). The most common indications for MPI included chest pain (39%,  $N = 29$ ), prior indeterminate stress testing (24%,  $N = 18$ ), screening study due to prior arterial switch or definite coronary artery abnormality (23%,  $N = 17$ ) or heart failure (22%,  $N = 16$ ). The majority of subjects had prior ischemic testing (73%,  $N = 55$ ), a median of 735 days prior to MPI (Table 2). At the time of MPI, treadmill exercise was most common form of stress (64%,  $N = 48$ ) followed by bike exercise (20%,  $N = 15$ ) and pharmacologic stress (16%,  $N = 12$ ). Details about associated cardiac anomalies, vascular risk factors, stress findings, and coronary artery imaging are provided in Supplemental material.

### Sequential Interpretation of MPI Imaging Findings

The majority of subjects (98.7%,  $N = 74$ ) underwent 1-day rest-stress imaging with SPECT (85%,  $N = 64$ ) or PET (15%,  $N = 11$ ). For SPECT, 5% were performed with CT-based attenuation correction and 8% with CZT SPECT. Rest/stress scans were normal in 56.0% (42/75 subjects). Rest/stress MPI was abnormal in 32 of 75 subjects (42.7%). One study was indeterminate. Fixed defects were present in 32.0% (24/75 subjects) and 25.0% (8/32 subjects) of the abnormal scans demonstrated reversible defects (partially or completely) suggesting ischemia.

The subpulmonary ventricle (most frequently the right ventricle) was normal in 53% ( $N = 39$ ), function was normal in 65% ( $N = 48$ ), and subpulmonary ventricle tracer uptake was normal in 34% ( $N = 25$ ). The mean systemic ventricular ejection fraction was normal at  $58 \pm 11.6\%$ .

The deidentified MPI images were interpreted in a sequential approach assessing stress-only images (to simulate a stress-first imaging strategy), stress/rest images, and stress/rest images taking into account the history of a VSD (Figure 2). Stress-only interpretation resulted in more 'probably abnormal' results compared to the stress/rest interpretation ( $P = 0.02$ ). By taking into account the ventricular septal defect, there were more 'normal' results than compared to stress-only imaging but this was not statistically significant ( $P = 0.09$ ).

Stress-only images were interpreted and normal (normal or probably normal) in 40.0% (30/75 subjects) eliminating the need for a rest study. The remaining 58.7% (44/75 subjects) had abnormal stress images necessitating a rest scan. One study was equivocal.

In order to assess if the perfusion defect could be attributable to the VSD, the deidentified rest/stress images were sequentially interpreted in the third batch with the knowledge about VSD repair. Of the 24 subjects with fixed defects, 11 subjects showed defects involving only the basal septum consistent with VSD. After exclusion of these defects potentially from VSD, 28.0% (21/75 subjects) still demonstrated abnormal scans, and 36.4% (8/22 patient) of the abnormal scans were ischemic.

## Radiation Dose

The radiotracer dose and the estimated effective radiation doses are presented on Table 3, Figure 3. Mean effective radiation dose for the overall cohort was  $8.1 \pm 2.8$  mSv, higher in adults compared to children under age 16 years ( $9.1 \pm 2.5$  mSv vs.  $6.2 \pm 2.4$  mSv,  $P < 0.0001$ ). Radiation dose was lowest for  $^{13}\text{N}$ -ammonia PET MPI (Figure 3). For  $^{99\text{m}}\text{Tc}$ -sestamibi SPECT scans, the mean effective radiation dose was  $8.7 \pm 2.3$  mSv for NaI SPECT,  $12.5 \pm 0.9$  mSv for SPECT/CT, and  $6.3 \pm 0.2$  mSv for CZT SPECT. For PET, the effective radiation dose was  $6.1 \pm 1.2$  mSv for  $^{82}\text{rubidium}$  and  $2.1 \pm 0.6$  mSv for  $^{13}\text{N}$ -ammonia. The mean effective radiation dose for rest and stress MPI reduced significantly after 2010 when new technology of CZT SPECT and PET was routinely incorporated in clinical practice:  $10.6 \pm 3.1$  mSv,  $N = 45$ , before 2010 vs  $8.4 \pm 3.0$  mSv,  $N = 30$ , for scans performed in 2010 or later.

An effective radiation dose of  $\leq 9$  mSv, as recommended by the American Society of Nuclear Cardiology in at least 50% of the studies,<sup>22</sup> was achieved in 61.3% of the subjects for complete rest and stress MPI (Figure 4a). Only subjects with  $^{99\text{m}}\text{Tc}$ -sestamibi NaI SPECT without weight-based imaging received a higher dose. With weight-based dosing, majority of children aged  $< 16$  years (91.7%, 22 of 24 subjects) received a radiation dose  $\leq 9$  mSv for rest and stress MPI; only two children received 9.3 mSv and 9.5 mSv dose, respectively. All rest and stress MPI studies performed with CZT SPECT or PET/CT resulted in radiation doses  $\leq 9.0$  mSv. If a stress-first imaging strategy were employed, all subjects with normal stress MPI would have received an effective radiation dose of  $\leq 9$  mSv (Figure 4b). Of subjects with abnormal stress MPI who would require a rest MPI for a diagnostic test, if a 2-day study were employed using rest dose on each day, the effective radiation dose in all of subjects would have been  $\leq 9$  mSv (Figure 4c).

When compared to traditional estimates of effective radiation dose, newer dose estimates from SNMMI radiation dosimetry tool which considers patient age and gender were higher particularly for children and women, but the results are otherwise very similar (Table 3). Representative examples of myocardial perfusion imaging in individuals with complex congenital heart disease are shown in Figures 5 and 6.

## DISCUSSION

To our knowledge, this study of 75 subjects is the largest published experience on ischemia evaluation by MPI in complex CHD. We found several notable findings in this study. The mean effective radiation dose from rest and stress MPI was highly variable and ranged from a dose of 1.4 mSv for  $^{13}\text{N}$ -ammonia PET study to 13.6 mSv for a test with  $^{99\text{m}}\text{Tc}$ -sestamibi SPECT. Rest and stress MPI with low radiation dose ( $< 9$  mSv) was feasible in all

subjects who underwent PET or CZT SPECT, and in most (93%) subjects who underwent weight-based dosing for  $^{99m}\text{Tc}$ -sestamibi. Stress-first MPI and 2-day equal dose rest and stress MPI could have resulted in  $< 9\text{mSv}$  radiation dose in all subjects. Based on our study findings, we propose the use of novel protocols, novel scanner technology, and novel image reconstruction software to minimize radiation dose from MPI in individuals with complex CHD (Figure 7).

Adult congenital heart disease guidelines suggest that imaging of patency of coronary arteries is reasonable in asymptomatic patients and physiologic testing of myocardial perfusion is reasonable in symptomatic individuals with transposition of the great arteries and prior arterial switch operation<sup>23</sup> due to the known risk of coronary ostial fibrointimal proliferation and kinking that can lead to ischemia and sudden cardiac death in some subjects.<sup>8,9</sup> This is reflected in our study with majority of subjects having transposition of the great arteries with arterial switch surgery, highlighting a need to develop systematic protocols for ischemia evaluation including low radiation dose MPI. Of the subjects who underwent coronary artery imaging following MPI, prior coronary artery translocation was one of the most common etiologies of significant coronary artery obstruction (Supplemental Table 3), suggesting these subjects may be a specific cohort who may be targeted for ischemia surveillance.

MPI is not typically the initial test of choice for ischemia evaluation in complex CHD. In our study, almost three quarters of subjects underwent exercise or stress echo prior to MPI. Exercise stress ECG testing was most commonly performed with positive or indeterminate results in 70% ( $N = 21$ ) of the subjects. Imaging may thus be required in conjunction with exercise ECG testing in majority of subjects with CHD requiring ischemic testing. Stress echo was performed prior to MPI in 18% ( $N = 10$ ) of subjects with positive or indeterminate results in the most subjects (80%,  $N = 8$ ), likely reflecting the challenges of stress echo interpretation in complex CHD and selective referral of subjects to MPI for confirmation of indeterminate findings.

Reducing lifetime radiation burden is a key priority, particularly for subjects with CHD. The effective radiation dose from rest and stress MPI in our study was variable and ranged from 1.4 mSv for  $^{13}\text{N}$ -ammonia PET to 13.6 mSv for a  $^{99m}\text{Tc}$ -sestamibi SPECT; estimated doses were slightly higher in women and children using age- and gender-specific radiation dose tool from SNMML. Radiation reduction strategies are essential to reduce the long-term health effects of the cumulative burden of ionizing radiation in individuals with CHD.<sup>10</sup> Recently described “best practices” for radiation reduction for MPI encourage avoidance of thallium, use of total effective radiation dose  $< 9\text{mSv}$ , stress-only imaging, use of camera-based dose reduction strategies (attenuation correction, multi-position imaging, advanced software), weight-based radiotracer dosing, and minimizing ‘shine through’ artifact by ensuring that the second injection performed on the same day is 3 times the dose of the first.<sup>24</sup> In our study, many of the radiation reduction strategies were followed including not using any thallium. Weight-based dosing of technetium was performed at the pediatric hospital and at the adult hospital since 2010 and ‘shine through’ artifact was avoided in all subjects. Radiation doses of  $< 9\text{mSv}$  were achieved in all of the CZT SPECT and PET/CT studies.



Stress-only imaging is recommended whenever feasible to reduce radiation dose.<sup>14,25</sup> If stress imaging is abnormal, rest imaging can be performed. In our study cohort of subjects with complex CHD, stress-only imaging would have been feasible in only 41%. Even when the MPI interpreter has access to detailed knowledge of the congenital heart disease anatomy and knowledge of the presence of absence of a VSD patch, a feature that can mimic a perfusion defect, only 58% of studies were interpreted as normal making a stress-only imaging strategy practical for less than half of subjects with complex CHD. Instead, a protocol of stress-first imaging, followed by a 2-day equal radiotracer dose rest study if needed, although cumbersome, may save substantial radiation dose in these young individuals, allow for effective radiation dose of 9 mSv for almost all subjects.

Camera-based dose reduction strategies using PET<sup>11</sup> and CZT SPECT<sup>26</sup> are known to reduce effective radiation dose in adult subjects undergoing MPI.<sup>15</sup> In this study, effective radiation dose for rest and stress MPI was < 8 mSv for all PET and for all CZT SPECT studies. Implementation of advanced imaging technology in the adult hospital reduced the effective radiation dose for MPI by 20% in complex CHD. With novel CZT SPECT technology and ultra-low radiation dose, further dose reduction to < 1 mSv for stress MPI is feasible.<sup>27</sup>

Hybrid MPI with low radiation dose CT for attenuation correction<sup>28</sup> generally results in improved image quality and increases the likelihood of performing stress-only imaging thereby lowering effective radiation doses. Hybrid MPI/CT images also have the potential to improve specificity of MPI interpretation in complex CHD by helping to identify the anatomic location of atypical outflow tracts or VSD patches or baffles which may help assess if there is an anatomical reason for a perfusion defect. However, our study was underpowered to address the added value of hybrid MPI/CT imaging in complex CHD; only 15% of subjects underwent PET/CT MPI and 5% underwent SPECT/CT.

## STRENGTHS AND LIMITATIONS

Despite the relatively small sample size compared to adult MPI studies, this study remains the largest published experience of MPI in complex CHD. Inclusion of subjects from an adult and a pediatric institution, use of several different scanner types, and a study period that spanned several years, allowed us to evaluate the entire spectrum of subjects from childhood to adulthood, and compare radiation doses between various radiotracers and scanners and temporal trends. In order to limit interobserver variability, all images were deidentified and reviewed systematically by an experienced investigator. Quantitative MPI analysis by software could not be used since no normal limits databases exist for complex CHD. Prospective data/testing for dyslipidemia or inquiring about a family history of coronary artery disease were lacking in the pediatric hospital medical records; however, coronary atherosclerosis was only a small component of the coronary pathology in this cohort.

## CONCLUSIONS

Radiation dose from MPI in complex CHD is highly variable and varies by the imaging protocol and the scanner used. Advanced imaging methods including CZT SPECT and PET MPI minimize radiation dose from MPI in individuals with complex CHD. For all SPECT and PET scanners, an imaging protocol of stress-first MPI followed by rest MPI if needed on another day provides the smallest effective radiation dose. Minimizing radiation dose may limit layered testing in at least some of these individuals with complex CHD and optimize effective evaluation of ischemia.

## Supplementary Material

Refer to Web version on PubMed Central for supplementary material.

## Disclosure

Sharmila Dorbala has received consulting fees from GE and research support from Pfizer. Ron Blankstein has received research support from Astellas Inc. and Amgen Inc. Marcelo F. DiCarli has received research support from Spectrum Dynamics and Gilead. Hicham Skali has received stock options in Optimize Rx for consulting role. Viviany R. Taqueti, Anne Marie Valente, Sara L. Partington, John Bruyere, Dillenia Rosica, Keri M. Shafer, Michael J. Landzberg, Neha Kwatra, and Frederick D. Grant have nothing to disclose.

## Abbreviations

<b>CHD</b>	Congenital heart disease
<b>CMR</b>	Cardiac magnetic resonance
<b>CZT</b>	Cadmium zinc telluride
<b>MPI</b>	Myocardial perfusion imaging
<b>NaI</b>	Sodium iodide
<b>PET</b>	Positron emission tomography
<b>SPECT</b>	Single-photon emission computed tomography
<b>VSD</b>	Ventricular septal defect

## References

1. Warnes CA, Liberthson R, Danielson GK, et al. Task force 1: The changing profile of congenital heart disease in adult life. *J Am Coll Cardiol*2001;37:1170–5. [PubMed: 11300418]
2. Marelli AJ, Mackie AS, Ionescu-Ittu R, Rahme E, Pilote L. Congenital heart disease in the general population: Changing prevalence and age distribution. *Circulation*2007;115(2):163–72. [PubMed: 17210844]
3. Deen JF, Krieger EV, Slee AE, et al. Metabolic syndrome in adults with congenital heart disease. *J Am Heart Assoc*2016;5:e001132. [PubMed: 26873680]
4. Giannakoulas G, Dimopoulos K, Engel R, et al. Burden of coronary artery disease in adults with congenital heart disease and its relation to congenital and traditional heart risk factors. *Am J Cardiol*2009;103:1445–50. [PubMed: 19427444]

5. Yalonetsky S, Horlick EM, Osten MD, Benson LN, Oechslin EN, Silversides CK. Clinical characteristics of coronary artery disease in adults with congenital heart defects. *Int J Cardiol*2013;164:217–20. [PubMed: 21807422]
6. Partington SL, Valente AM, Landzberg M, Grant F, Di Carli MF, Dorbala S. Clinical applications of radionuclide imaging in the evaluation and management of patients with congenital heart disease. *J Nucl Cardiol*2016;23:45–63. [PubMed: 26129940]
7. Morray BH, McElhinney DB, Cheatham JP, et al. Risk of coronary artery compression among patients referred for transcatheter pulmonary valve implantation: a multicenter experience. *Circ Cardiovasc Interv*2013;6:535–42. [PubMed: 24065444]
8. Bonnet D, Bonhoeffer P, Piechaud JF, et al. Long-term fate of the coronary arteries after the arterial switch operation in newborns with transposition of the great arteries. *Heart*1996;76:274–9. [PubMed: 8868989]
9. Tanel RE, Wernovsky G, Landzberg MJ, Perry SB, Burke RP. Coronary artery abnormalities detected at cardiac catheterization following the arterial switch operation for transposition of the great arteries. *Am J Cardiol*1995;76:153–7. [PubMed: 7611150]
10. Hill KD, Frush DP, Han BK, et al. Radiation safety in children with congenital and acquired heart disease: a scientific position statement on multimodality dose optimization from the image gently alliance. *JACC Cardiovasc Imaging*2017;10:797–818. [PubMed: 28514670]
11. Di Carli MF, Dorbala S, Meserve J, El Fakhri G, Sitek A, Moore SC. Clinical myocardial perfusion PET/CT. *J Nucl Med*2007;48:783–93. [PubMed: 17475968]
12. DePuey EG, Ata P, Wray R, Friedman M. Very low-activity stress/high-activity rest, single-day myocardial perfusion SPECT with a conventional sodium iodide camera and wide beam reconstruction processing. *J Nucl Cardiol*2012;19:931–44. [PubMed: 22777525]
13. DePuey EG. Advances in SPECT camera software and hardware: currently available and new on the horizon. *J Nucl Cardiol*2012;19(3):551–81 quiz 585. [PubMed: 22456968]
14. Chang SM, Nabi F, Xu J, Raza U, Mahmarian JJ. Normal stress-only versus standard stress/rest myocardial perfusion imaging: similar patient mortality with reduced radiation exposure. *J Am Coll Cardiol*2010;55:221–30. [PubMed: 19913381]
15. Dorbala S, Blankstein R, Skali H, et al. Approaches to reducing radiation dose from radionuclide myocardial perfusion imaging. *J Nucl Med*2015;56:592–9. [PubMed: 25766891]
16. Kuebler JD, Chen MH, Alexander ME, Rhodes J. Exercise performance in patients with D-loop transposition of the great arteries after arterial switch operation: Long-term outcomes and longitudinal assessment. *Pediatr Cardiol*2016;37:283–9. [PubMed: 26439943]
17. Cerqueira MD, Weissman NJ, Dilsizian V, et al. Standardized myocardial segmentation and nomenclature for tomographic imaging of the heart. A statement for healthcare professionals from the Cardiac Imaging Committee of the Council on Clinical Cardiology of the American Heart Association. *J Nucl Cardiol*2002;9:240–5. [PubMed: 11986572]
18. Hachamovitch R, Berman DS, Kiat H, et al. Exercise myocardial perfusion SPECT in patients without known coronary artery disease: incremental prognostic value and use in risk stratification. *Circulation*1996;93:905–14. [PubMed: 8598081]
19. Hachamovitch R, Hayes SW, Friedman JD, Cohen I, Berman DS. A prognostic score for prediction of cardiac mortality risk after adenosine stress myocardial perfusion scintigraphy. *J Am Coll Cardiol*2005;45:722–9. [PubMed: 15734617]
20. Cohen HA, Baird MG, Rouleau JR, et al. Thallium 201 myocardial imaging in patients with pulmonary hypertension. *Circulation*1976;54:790–5. [PubMed: 975475]
21. Mannting F, Zabrodina YV, Dass C. Significance of increased right ventricular uptake on <sup>99m</sup>Tc-sestamibi SPECT in patients with coronary artery disease. *J Nucl Med*1999;40:889–94. [PubMed: 10452302]
22. Dorbala S, Di Carli MF, Delbeke D, et al. SNMMI/ASNC/SCCT guideline for cardiac SPECT/CT and PET/CT 1.0. *J Nucl Med*2013;54:1485–507. [PubMed: 23781013]
23. Stout KK, Daniels KG, Aboulhosn JA, Bozkurt B, Broberg CS, Colman JM, Crumb SR, Dearani JA, Fuller S, Gurvitz M, Khairy P, Landzberg MJ, Saidi A, Valente AM, Van Hare GF. AHA/ACC Guideline for the Management of Adults with congenital heart disease. *J Am Coll Cardiol*2018;18:S0735–1097.

24. Einstein AJ, Pascual TN, Mercuri M, et al. Current worldwide nuclear cardiology practices and radiation exposure: results from the 65 country IAEA Nuclear Cardiology Protocols Cross-Sectional Study (INCAPS). *Eur Heart J* 2015;36:1689–96. [PubMed: 25898845]
25. Iskandrian AE. Stress-only myocardial perfusion imaging a new paradigm. *J Am Coll Cardiol* 2010;55:231–3. [PubMed: 19913382]
26. Einstein AJ, Johnson LL, DeLuca AJ, et al. Radiation dose and prognosis of ultra-low-dose stress-first myocardial perfusion SPECT in patients with chest pain using a high-efficiency camera. *J Nucl Med* 2015;56:545–51. [PubMed: 25745089]
27. Einstein AJ, Blankstein R, Andrews H, et al. Comparison of image quality, myocardial perfusion, and left ventricular function between standard imaging and single-injection ultra-low-dose imaging using a high-efficiency SPECT camera: the MILLI-SIEVERT study. *J Nucl Med* 2014;55:1430–7. [PubMed: 24982439]
28. Patton JA, Turkington TG. SPECT/CT physical principles and attenuation correction. *J Nucl Med Technol* 2008;36:1–10. [PubMed: 18287196]
29. Abbott BG, Case JA, Dorbala S, et al. Contemporary Cardiac SPECT imaging-innovations and best practices: An information statement from the American Society of Nuclear Cardiology. *J Nucl Cardiol* 2018;25:1847–60. [PubMed: 30143954]
30. Dorbala S, Ananthasubramaniam K, Armstrong IS, et al. Single photon emission computed tomography (SPECT) Myocardial Perfusion Imaging Guidelines: Instrumentation, acquisition, processing, and interpretation. *J Nucl Cardiol* 2018;25:1784–846. [PubMed: 29802599]
31. Henzlova MJ, Duvall WL, Einstein AJ, Travin MI, Verberne HJ. ASNC imaging guidelines for SPECT nuclear cardiology procedures: Stress, protocols, and tracers. *J Nucl Cardiol* 2016;23:606–39. [PubMed: 26914678]

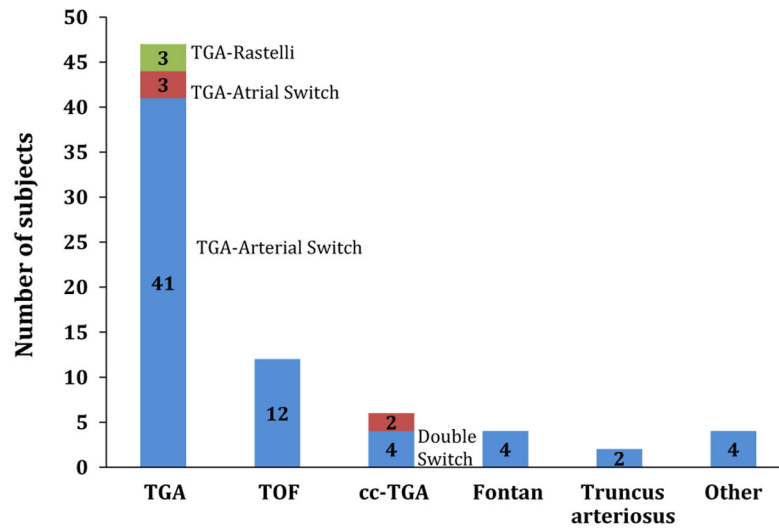


**Figure 1.** Distribution of the underlying anatomic complex congenital heart disease diagnosis. The most common underlying congenital heart disease was transposition of great arteries with arterial switch operation. *TGA*, transposition of great arteries; *TOF*, Tetralogy of Fallot; *cc-TGA*, congenitally corrected transposition of great arteries.

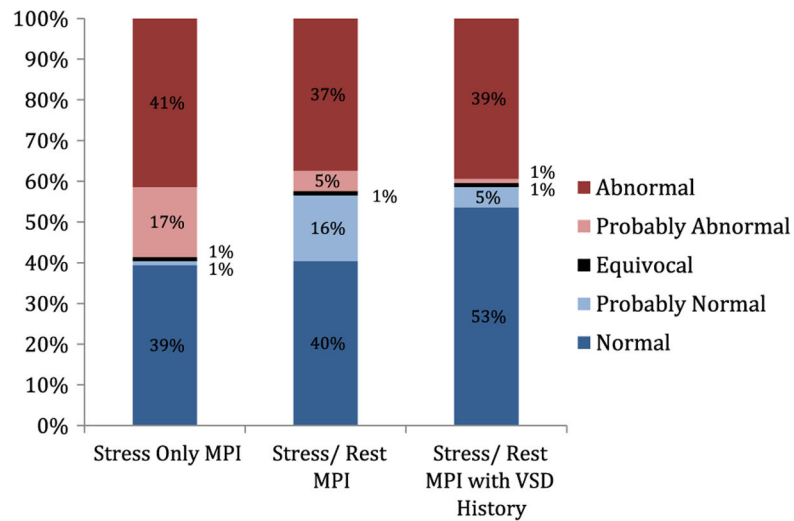


**Figure 2.**

Sequential interpretation of myocardial perfusion images. Images of all 75 subjects were sequentially interpreted using stress-only, stress/rest, and stress/rest images and taking into account the presence or absence of a history of a ventricular septal defect. Stress-only interpretation resulted in more 'probably abnormal' results compared to the stress/rest interpretation. By taking into account a history of ventricular septal defect, there was a trend toward more 'normal' results. *MPI*, myocardial perfusion imaging; *VSD*, ventricular septal defect.

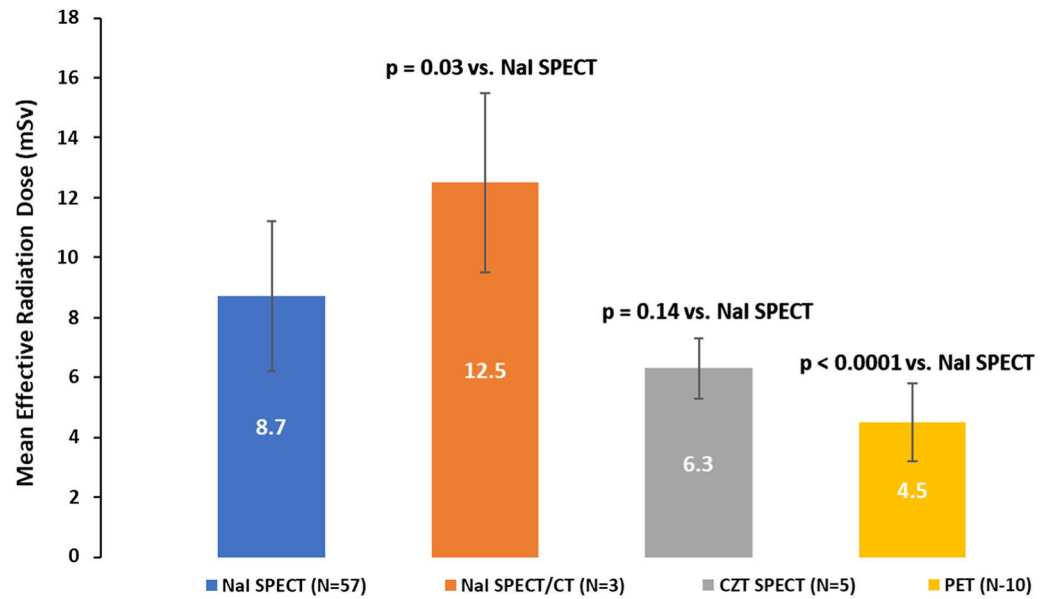


**Figure 3.**

Total estimated effective radiation dose for rest/stress MPI by radiotracer and scanner type. Total effective radiation dose was lowest for PET MPI. *MPI*, myocardial perfusion imaging; *NaI*, sodium iodide; *CZT*, cadmium zinc telluride.

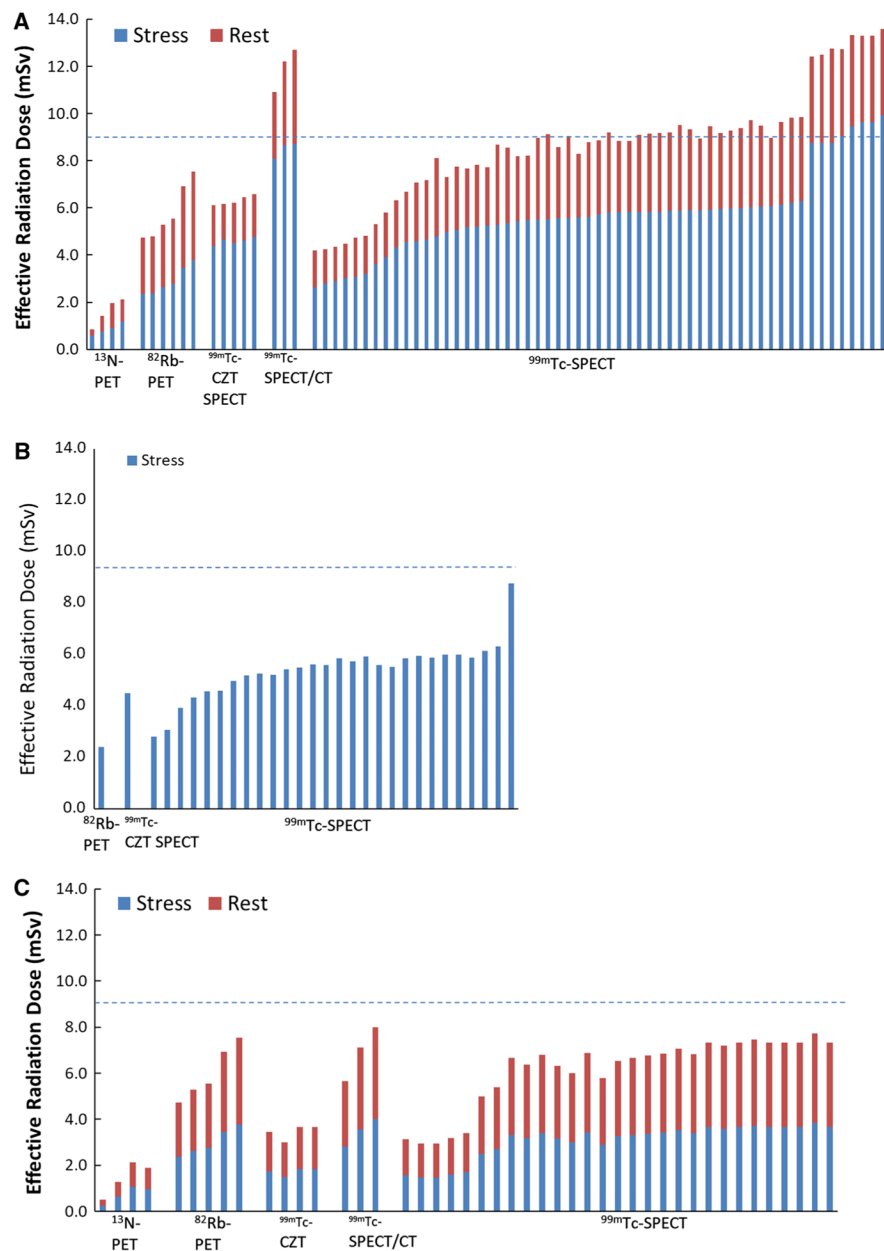


**Figure 4.**

Estimated effective radiation dose from various myocardial perfusion imaging (MPI) protocols. Rest/stress MPI (A), stress-only MPI (B), 2-day rest/stress MPI (C). The dotted line represents 9 mSv threshold for low radiation dose. All subjects who underwent  $^{99\text{m}}\text{Tc}$ -SPECT with CZT scanners, or PET MPI received less than 9 mSv dose for rest and stress MPI. Likewise stress-only and 2-day rest/stress equal dose MPI were estimated to result in < 9 mSv effective dose. \*Doses estimated for two equal rest radiotracer doses. *Rb*, rubidium; *CZT*, cadmium zinc telluride; *Tc*, technetium.



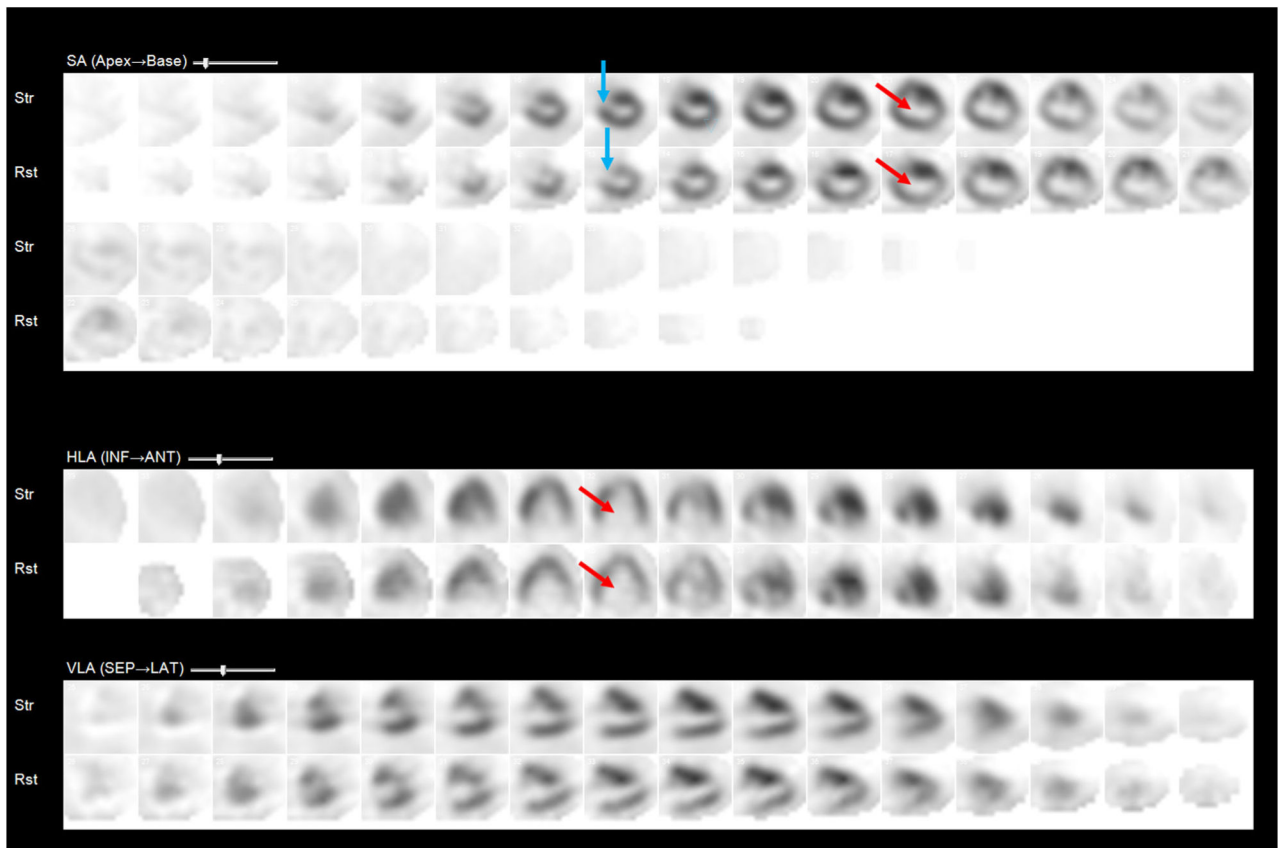


**Figure 5.**

Representative example of a myocardial perfusion image from a 34-year-old woman with repaired ventricular septal defect (VSD). Rest and stress myocardial perfusion images demonstrate a severe fixed perfusion defect in the entire septum (red arrow) consistent with known prior VSD repair surgery. The blue arrow points to a small apical anterior wall infarction.

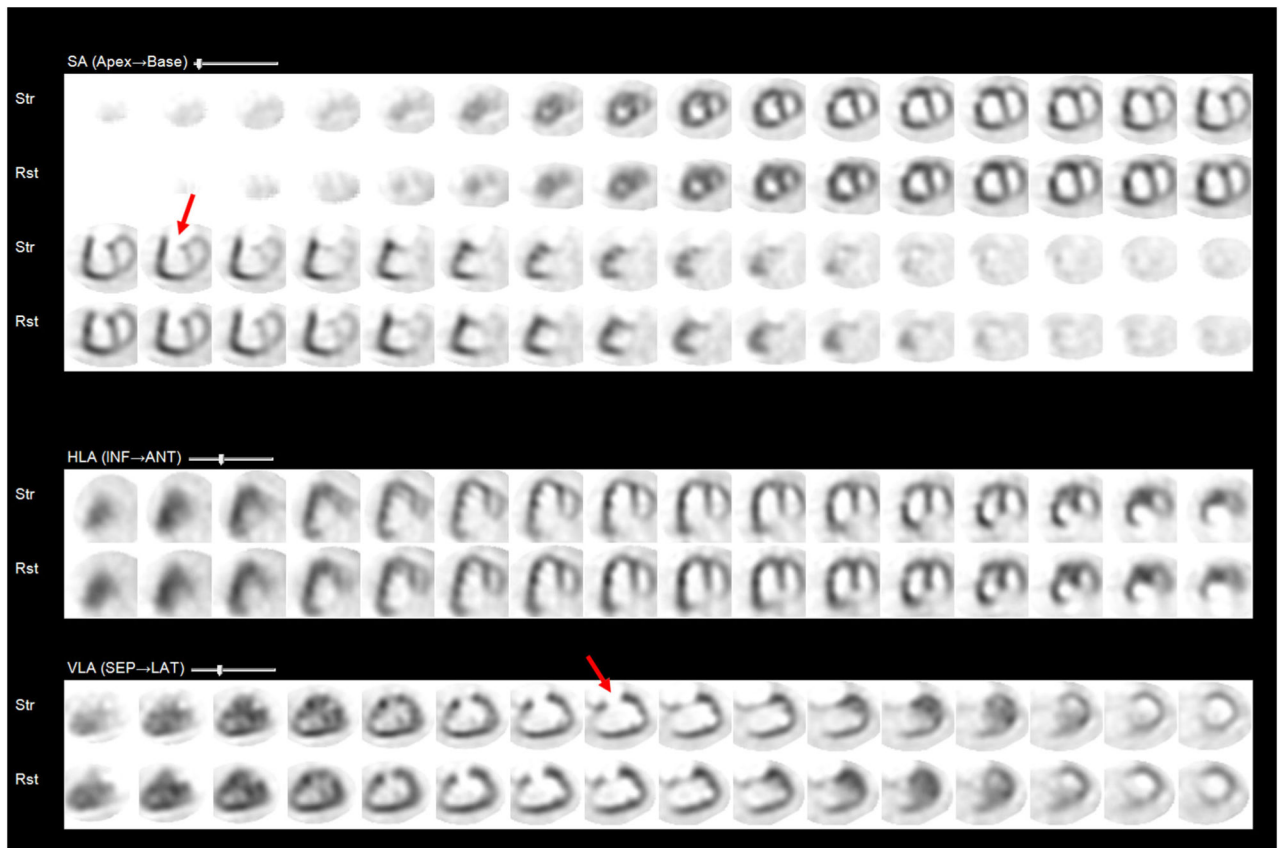


**Figure 6.**

Representative example of a myocardial perfusion image from a 15-year-old boy with a systemic right ventricle. Rest and stress myocardial perfusion images demonstrate a right-sided systemic right ventricle that is enlarged and nearly normally perfused. The apparent perfusion defect at the base of the anterior wall of the right ventricle (arrow) represents the take-off of the aorta which is an expected finding.

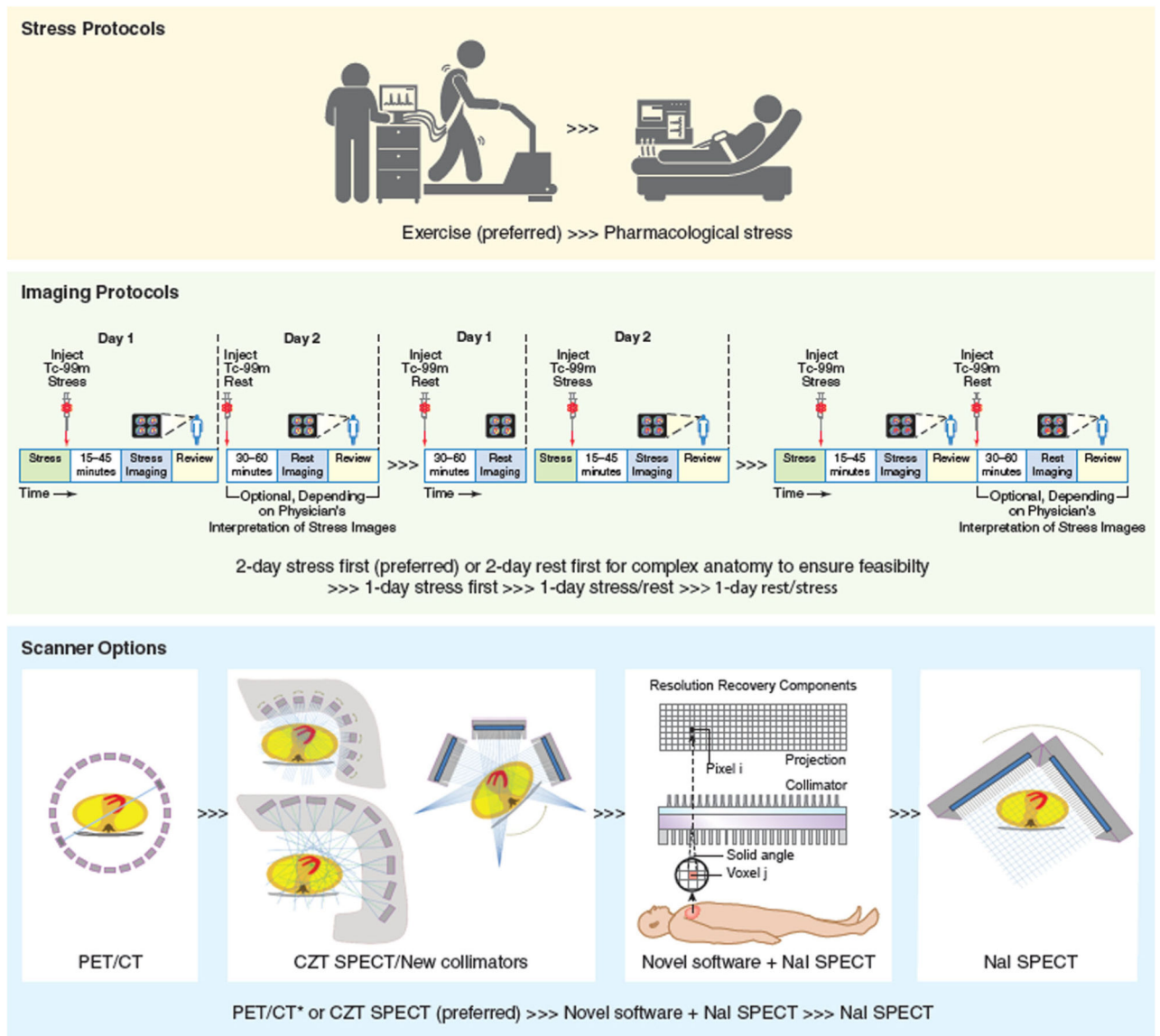


**Figure 7.**

Options for low radiation dose imaging in complex congenital heart disease patients. For the evaluation of complex congenital heart disease, exercise stress is typically preferred over pharmacological stress to enable detection of ischemia from compressive physiologies. To perform low radiation dose imaging: (1) 2-day protocols are preferred over 1-day protocols; (2) stress-first protocol is preferred; rest first may be considered when cardiac anatomy is complex (to evaluate feasibility of interpretable imaging); (3) 1-day stress/rest protocols or 1-day rest/stress protocols are least preferred. For scanners, PET is preferred for pharmacological stress and for exercise stress when if  $^{13}\text{N}$ -ammonia is available; for SPECT, (1) CZT SPECT, (2) novel collimator SPECT/novel software (iterative reconstruction, resolution recovery, and noise reduction) with NaI SPECT, and (3) NaI SPECT with filtered back projection reconstruction are options in that order. Figure by Wendy B. Jakelow with

parts of figure reproduced with permission (stress protocols from © Can Stock Photo Inc. / Leremy; imaging protocols and scanner from references).<sup>29-31</sup>.

Author Manuscript

Author Manuscript

Author Manuscript

Author Manuscript

Table 1.

## Baseline characteristics of the study cohort

	N = 75
<b>Demographics</b>	
Age at ischemia study, (median, IQR)	18.6 years (15.1–28.4 years)
Age at arterial switch operation, (median, IQR)	6 days (3–15.5 days)
Male N (%)	49 (65.3%)
Body mass index Kg/m <sup>2</sup> (mean ± SD)	22.8 ± 13.8
<b>Major type of CHD, N (%)</b>	
Time since corrective surgery-median (IQR)	17 years (14–22)
Time since coronary reimplantation-Median (IQR)	17 years (13–20)
<b>Associated CHD anomalies, N (%)</b>	
Ventricular septal defect N (%)	35 (47.3%)
Systemic right ventricle N (%)	7 (9.5%)
Right-sided systemic ventricle N (%)	8 (10.8%)
Single ventricle N (%)	4 (5.3%)
<b>Prior correction of CHD, N (%)</b>	
TGA with arterial switch procedure <sup>a</sup>	45 (60.0%)
TGA with atrial switch procedure <sup>a</sup>	5 (6.7%)
TGA with Rastelli procedure	3 (4.0%)
Coronary reimplantation	45 (60.0%)
Ventricular septal defect patch	28 (37.3%)
Right ventricle-pulmonary artery conduit	9 (12.0%)
Ventricular baffle	4 (5.3%)
<b>Coronary artery abnormalities, N (%)</b>	
History coronary artery disease	8 (10.7%)
Coronary artery reimplantation	45 (60.0%)
Coronary artery compression	9 (12.0%)
Single coronary artery	10 (13.3%)
Hypoplastic coronary artery	2 (2.6%)

Reason for study, N (%) <sup>b</sup>		N = 75
Chest pain		29 (39.2%)
Dyspnea/CHF/viability		16 (21.6%)
Prior testing abnormal/indeterminate		18 (24.3%)
Screening (TGA, s/p arterial switch, or definite coronary abnormality)		17 (23%)
Rest electrocardiogram, N (%) <sup>b</sup>		
Normal		8 (10.8%)
Right bundle branch block		25 (33.8%)
Paced		9 (12.2%)
Baseline ST-T wave changes		56 (75.7%)
Right ventricular hypertrophy		9 (12.2%)

*SD*, standard deviation; *IQR*, interquartile range; *CHF*, congestive heart failure; *TGA*, transposition of great arteries

<sup>a</sup>Includes subjects with congenitally corrected transposition of the great arteries with a double-switch surgery (atrial and arterial switch)

<sup>b</sup>Numbers do not add up to 100% as diagnosis could not be ascertained in all subjects

**Table 2.**

## Prior non-invasive coronary evaluation

	N (%)
Any prior ischemia testing	55 (73.3)
Median time since prior ischemia testing	735 days
Stress electrocardiogram (ECG)	30 (55%)
Normal	9 (30%)
Abnormal	3 (10%)
Indeterminate	18 (60%)
Stress echocardiogram	10 (18%)
Normal	2 (20%)
Abnormal	5 (50%)
Indeterminate	3 (30%)
Stress/rest SPECT MPI	15 (27%)
Normal	11 (73%)
Abnormal	2 (13%)
Indeterminate	2 (13%)
Prior coronary angiography ever	62 (84%)

Author Manuscript

Author Manuscript

Author Manuscript

Author Manuscript

Table 3.

Myocardial perfusion imaging technique and estimated radiation dose

Radiotracer dose (mCi)	Estimated effective radiation dose (mSv)											
	Radiation dose estimates					Age/sex adjusted radiation dose estimates (SNMMI Tool)						
	Rest (mCi)	Stress (mCi)	Total (mCi)	Rest (mSv)	Stress (mSv)	Total (mSv) Including CT	Rest (mSv)	Stress (mSv)	Total (mSv) Including CT	Rest (mSv)	Stress (mSv)	Total (mSv) Including CT
SPECT: 85.1% (65)												
<sup>99m</sup> Tc-NaI scanner no AC, 87.7% (N = 57)	8.9 ± 2.1	19.7 ± 5.9	29.6 ± 7.7	3.0 ± 0.7	5.8 ± 1.7	8.7 ± 2.3	3.6 ± 0.8	6.8 ± 1.9	10.5 ± 2.5			
<sup>99m</sup> Tc-NaI scanner with CTAC, 4.6% (N = 3)	10.4 ± 1.8	29.0 ± 1.2	39.4 ± 2.9	3.5 ± 0.6	8.5 ± 0.3	12.5 ± 0.9	4.3 ± 1.3	10.0 ± 1.7	14.9 ± 3.0			
<sup>99m</sup> Tc-CZT no AC, 7.7% (N = 5)	5.2 ± 0.4	15.7 ± 0.5	20.9 ± 0.7	1.7 ± 0.1	4.6 ± 0.1	6.3 ± 0.2	2.0 ± 0.3	5.3 ± 0.7	7.4 ± 1.0			
PET: 14.9% (10)												
<sup>82</sup> Rubidium dose, 60% (N = 6)	46.1 ± 9.3	46.1 ± 9.3	92.2 ± 18.6	2.9 ± 0.6	2.9 ± 0.6	6.1 ± 1.2						
<sup>13</sup> N-ammonia dose, 40% (N = 4)	7.3 ± 3.6	8.6 ± 2.5	15.9 ± 5.8	0.7 ± 0.4	0.9 ± 0.3	2.1 ± 0.6						

AC, attenuation correction; CZT, cadmium zinc telluride; CT, computed tomography; NaI, Sodium iodide; PET, positron emission tomography; <sup>99m</sup>Tc, <sup>99m</sup>Technetium